Integrated Sensing Framework for 3D Mapping in Outdoor Navigation

R. Katz, N. Melkumyan, J. Guivant, T. Bailey, J. Nieto and E. Nebot

ARC Centre of Excellence for Autonomous Systems

Australian Centre for Field Robotics

The University of Sydney, Australia

{r.katz}@cas.edu.au

Abstract— Although full 3D navigation and mapping is recognized as one of the most important challenges for autonomous navigation, the lack of robust sensors, providing 3D information in real time, has burdened the progress in this direction. This paper presents our ongoing work towards the deployment of an integrated sensing system for 3D mapping in outdoor environments. We first describe a 3D data acquisition architecture based on a standard 2D laser. Techniques for registering scans using a scan matching procedure and for estimating the errors are then introduced. We finally present results showing the performance of the proposed architecture in real outdoor environments by means of the integration of the 3D scans with dead reckoning and inertial measurement unit (IMU) information.

I. INTRODUCTION

In the past few years significant work has been carried out in navigation and simultaneous localization and mapping (SLAM) [1], [2], [3]. The vehicle position is evaluated by combining the data received from the internal sensors such as encoders and external sensors such as lasers, radar or GPS. Laser has become very popular in SLAM applications [4], [5], [6]. Although this sensor is able to obtain 2D range and bearing scans of the environment fast and accurately, for many 2D navigation applications –specially in outdoor environments– this might not provide enough information. Full 3D navigation and mapping in unstructured all terrain environments is recognized as one of the most important challenges for autonomous navigation. The lack of robust sensors capable of providing rich 3D information in real time has been one of the main limiting factors in this sense. Sensory procedures in indoor environments are usually simplified since the complexity of the problem can be reduced. In this context the utilization of 2D laser range scanner is usually sufficient for SLAM purposes. However, outdoor environments present very different challenges [7] and we need to rely on more complex sensory mechanisms, such as the one provided by a 3D laser range scanner.

In this work we discuss our progress towards the deployment of a 3D sensory system for environmental sensing and navigation in outdoor environments. The developed 3D data acquisition architecture is first introduced in Section II. It is clear that, for almost any autonomous task, the robot must know its position within the environment. Dead reckoning sensors generate an unbounded error that needs to be compensated to obtain a more accurate estimate of the robot position. One way to achieve this is to match range scans [8] taken at different locations at different times in the environment, and to update the position estimation according to the matching result. Moreover, an accurate registration procedure to assemble 3D scans into one consistent global representation is useful for mapping. Therefore, Section III presents the basic concepts for the registration of the 3D scans obtained with the 3D laser range scanner described in Section II. The approach is further improved using initial poses provided by the integration of steering-velocity encoders and IMU, reducing the convergence times for the registration procedure while minimizing the risks of reaching local minima.

Some information about the uncertainty of the registration is probably as important as an accurate registration method. An estimation of the registration errors becomes particularly relevant in outdoor environments, where difficult setting configuration (long walls, corridors, repetitive patterns such as trees or cars, etc.) might "confuse" the registration procedure and lead to a high uncertain alignment. Moreover, the uncertainty of the registration is necessary to use the estimated 3D registration pose in a probabilistic framework (such as a Kalman filter) with i nformation provided by other sensors. The approach proposed in [9] for the estimation of the registration errors is then described in Section IV. Experimental results of the 3D data acquisition architecture are presented in Section V. We illustrate the performance of the system by showing images of the obtained 3D scans taken in real world outdoor environment, together with both the 3D registration poses and the corresponding estimation of the registration errors. Conclusions and future work are finally discussed in Section VI.

II. DESCRIPTION OF THE 3D DATA ACQUISITION ARCHITECTURE

We have developed a 3D data acquisition architecture built on the basis of a 2D Sick LMS-200 [10] laser scanner and an Amtec PowerCube PR090 servo motor. The images in Figure 1 show the 3D laser scanner, together with images of the system mounted on top of the research vehicle and the 3D coordinate frame. The total time for a complete 360° scan is about 2 secs.

The Sick LMS-200 laser scanner can obtain a 180 degree scan of the environment in 13 and 26 msec with 1 and 0.5 degree resolution respectively. An additional servo mechanism enables the system to capture the other dimension. The maximum range of the 3D scanner is approximately 80m with 1 cm accuracy. In order to achieve high data rates a dedicated hardware/software system is required to read the data at 500Kb through a RS422 interface.

The control of the 3D scanner system is done with a dedicated PC104 system running under QNX operating system [11]. A standard Xtreme/104 Opto board with 8Mhz oscillator is used to get the non standard serial speed of (500000bps). The sensor system can be programmed by the user in order to scan with a selected resolution, speed, and angle span. It then broadcasts raw laser/orientation data with the appropriate time-stamps through a standard ethernet interface. With this mechanism a client can be written to use this data using any other operating system. The same approach is used to acquire data and time-stamp from the other sensors in the research vehicle.

III. 3D REGISTRATION USING SCAN MATCHING

In this section we present the basic concepts for registation of 3D scans. Let $P = \{\mathbf{b}_i\}$ be a measurement data point set containing N_b 3D points, and a model point set $X = \{\mathbf{a}_i\}$ considered fixed and containing N_a 3D points. The goal of the registration is to find a transformation vector to align the data points of P to the model points of X. This transformation is composed by a 3D translation and rotation, such that it can be characterized by the six parameter vector $\mathbf{z} = [x, y, z, \alpha, \beta, \gamma]^T$.

In general, the general error metric to be minimized takes the form:

$$E(\mathbf{z}) = \sum_{i=1}^{N_b} \|\mathbf{a}_i - (\mathbf{R}\mathbf{b}_i + \mathbf{T})\|^2, \qquad (1)$$

where each of the $\mathbf{b}_i$ in the measurement data points (N_b) corresponds to the nearest point $\mathbf{a}_i$ in the model set, $\mathbf{R}$ is the rotation matrix and $\mathbf{T}$ is the translation vector, these two ($\mathbf{R},\mathbf{T}$) defining the registration vector $\mathbf{z} = [x, y, z, \alpha, \beta, \gamma]^T$. Instead of calculating the transformation ($\mathbf{R},\mathbf{T}$) directly in the original parameter space $\mathbf{z}$ it is convenient to use the quaternion based method presented in [12], where the transformation is expressed in terms of the vector $\mathbf{q} = [q_0, q_1, q_2, q_3, q_4, q_5, q_6]^T$. The unit quaternion is a four vector $\mathbf{q_R} = [q_0, q_1, q_2, q_3]^T$, where $q_0 \geq 0$, and $q_0^2 + q_1^2 + q_2^2 + q_3^2 = 1$. The 3×3 rotation matrix $\mathbf{R}$ generated by a unit quaternion is then calculated according to the following scheme:

$$\mathbf{R} = \begin{bmatrix} r_{11} & r_{12} & r_{13} \\ r_{21} & r_{22} & r_{23} \\ r_{31} & r_{32} & r_{33} \end{bmatrix}, \qquad (2)$$

with:

$$
\begin{aligned}
r_{11} &= q_0^2 + q_1^2 - q_2^2 - q_3^2 \\
r_{12} &= 2(q_1 q_2 - q_0 q_3) \\
r_{13} &= 2(q_1 q_3 + q_0 q_2) \\
r_{21} &= 2(q_1 q_2 + q_0 q_3) \\
r_{22} &= q_0^2 + q_2^2 - q_1^2 - q_3^2 \\
r_{23} &= 2(q_2 q_3 - q_0 q_1) \\
r_{31} &= 2(q_1 q_3 - q_0 q_2) \\
r_{32} &= 2(q_2 q_3 + q_0 q_1) \\
r_{33} &= q_0^2 + q_3^2 - q_1^2 - q_2^2.
\end{aligned}
$$

If this rotation is characterized by $Z - Y - X$ Euler angles, the three angles $[\alpha, \beta, \gamma]$ can be obtained as follows:

$$
\begin{aligned}
\alpha &= atan2(r_{21}/\cos\beta, r_{11}/\cos\beta) \\
\beta &= atan2(-r_{31}, \sqrt{r_{11}^2 + r_{21}^2}) \\
\gamma &= atan2(r_{32}/\cos\beta, r_{33}/\cos\beta). \qquad (3)
\end{aligned}
$$

The translation $\mathbf{T}$ is given by the vector:

$$\mathbf{T} = [x, y, z]^T = [q_4, q_5, q_6]^T. \qquad (4)$$

The ICP algorithm can be stated as in [13], [8] as follows:
- The data point set P with N_b points $\mathbf{b_i}$ and the model point set X with N_a points $\mathbf{a_i}$ are given.
- The iteration is initialized by setting an initial pose $\mathbf{q}_0 = [1, 0, 0, 0, 0, 0, 0]^T$, $P = P_0$ and $k = 0$. The registration vectors are defined relative to the initial data set P_0 so that the final registration represents the complete transformation. The next three steps 1, 2 and 3 are repeated until convergence within certain tolerance (determined by a least-mean-squared residual threshold), or indicated by a fixed number of iterations.
  1) Each point $\mathbf{b}_i$ in P_0 is transformed to $P_k = \{\mathbf{R}\mathbf{b}_i + \mathbf{T}\}$ using the current pose estimate $\mathbf{q}_k$ and the expressions in (2) and (4).
  2) Each transformed point in P_k is associated to its nearest neighbor in X.
  3) The associated pairs are used to calculate the relative pose $\mathbf{q}_{k+1}$ that minimizes the least-mean-squared error (1) between the associated points.

The final registration transformation is obtained upon convergence from $\mathbf{q}_{k+1}$ using (2)-(4).

IV. ESTIMATION OF THE REGISTRATION ERRORS

In general not only an accurate matching is important, but also a sound measure of the quality of the matching, i.e., the accuracy of the estimated 3D pose. The approach taken in [14] shows how a covariance matrix can be estimated directly from the corresponding pair of points. This estimation is based on the assumption that the algorithm always finds the same physical point in the measurement data point set and the model point set. This assumption can be easily violated when the
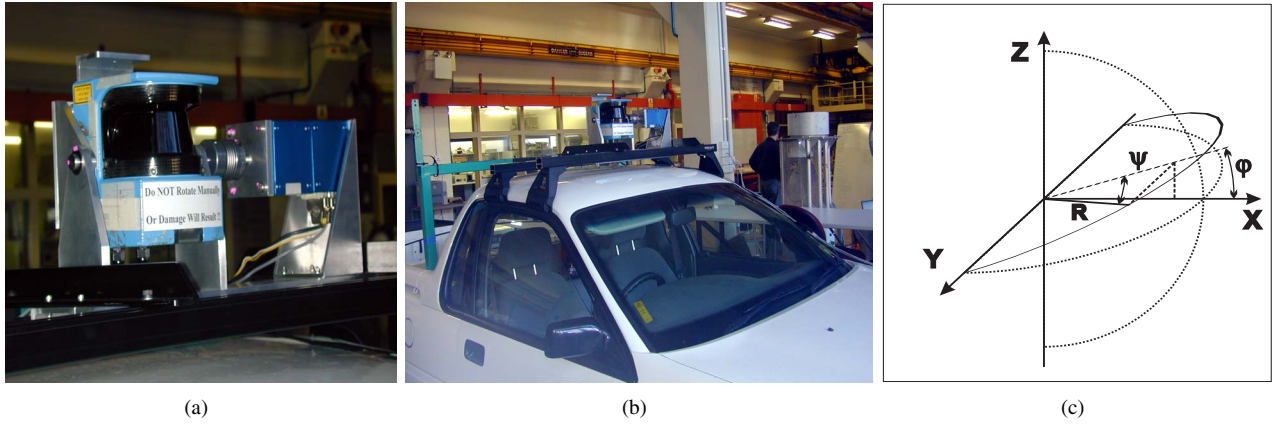
Fig. 1. Images showing the 3D data acquisition architecture. 3D laser range scanner in (a), system mounted on the research vehicle in (b), and coordinate frame of the 3D system in (c).

environment lacks of complex structure or when it contains repetitive patterns.

We choose for the estimation of the registration error the approach described in [9]. This procedure considers the uncertainty given by the environment layout and thus provides a more accurate estimation for the covariance matrix. Its basic concepts are more easily described if we rewrite (1) as:

$$E(\mathbf{z}) = (\mathbf{A} - M\mathbf{z})^T(\mathbf{A} - M\mathbf{z}), \qquad (5)$$

where $\mathbf{A}$ contains the model points $\mathbf{a}_i$, M is the observation matrix, and $\mathbf{z}$ is the registration vector. The observation matrix M ([15], [16]) is defined to relate errors in the transformation parameters to dimensional errors of the measurement point, as follows:

$$\epsilon = M\delta\mathbf{t},$$

with $\epsilon = [\epsilon_1, \epsilon_2, \ldots, \epsilon_{N_b}]^T$ the vector containing the dimensional errors, $\delta\mathbf{t} = [\delta t_1, \delta t_2, \delta t_3, \delta t_4, \delta t_5, \delta t_6]^T$ the vector containing the errors in each transformation parameter, and M defined as in [17] as:

$$M = \begin{bmatrix} n_1^x & n_1^y & n_1^z & -(\mathbf{n}_1 \times \mathbf{b}_1)^T \\ n_2^x & n_2^y & n_2^z & -(\mathbf{n}_2 \times \mathbf{b}_2)^T \\ \ldots & \ldots & \ldots & \ldots \\ n_{N_b}^x & n_{N_b}^y & n_{N_b}^z & -(\mathbf{n}_{N_b} \times \mathbf{b}_{N_b})^T \end{bmatrix}, \qquad (6)$$

with $\mathbf{b}_i$ the ith measurement point and $\mathbf{n}_i = [n_i^x, n_i^y, n_i^z]^T$ the normal vector at the ith measurement point.

The optimal state of (5) for the parameter vector $\mathbf{z}$ and $cov(\mathbf{z})$ are according to [18] as follows:

$$\mathbf{z} = (M^T M)^{-1} M^T A \qquad (7)$$
$$cov(\mathbf{z}) = (M^T M)^{-1}\sigma^2 \qquad (8)$$

An unbiased estimate of σ^2 can be calculated as:

$$\hat{\sigma}^2 = \frac{\hat{E}(\mathbf{z})}{n - k - 1} \qquad (9)$$

where $\hat{E}(\mathbf{z})$ is the minimized error for (5) at the found registration vector $\mathbf{z}$, n is the number of point matches of the registration and k is the number of estimated parameters.

A double differentiation of (5) gives the Hessian matrix H, as:

$$H = \frac{dE^2(\mathbf{z})}{d\mathbf{z}^2} = 2M^T M \Rightarrow M^T M = \frac{1}{2}H. \qquad (10)$$

Then, by combining (8), (9) and (10) the covariance $cov(\mathbf{z})$ becomes:

$$cov(\mathbf{z}) = \left(\frac{1}{2}H\right)^{-1}\hat{\sigma}^2. \qquad (11)$$

Once the scan matching algorithm has found the registration vector $\mathbf{z}$, each of the elements in the Hessian matrix H can be estimated. It is clear that for the case of a complete 3D registration with $\mathbf{z} = [x, y, z, \alpha, \beta, \gamma]^T$, the Hessian H is a 6×6 matrix, with the components corresponding to the second order partial derivatives. The calculation of the elements of H is done by first translating and rotating the measurement data point set of the actual scan; and then letting the registration algorithm find again the corresponding pair of points for the transformation, now affected by small perturbations in each of the parameters of the registration. In other words, the elements of the Hessian matrix H are calculated as follows:

1) Translate and rotate the measurement data point set of the actual scan according to the found registration vector $\mathbf{z}$ plus a small perturbation $\delta\mathbf{z} = [\delta x, \delta y, \delta z, \delta\alpha, \delta\beta, \delta\gamma]^T$.
2) Find the new corresponding pair of points in the model set point and in the modified transformed measurement data point set of the actual scan.
3) Calculate (5) based on the new corresponding pairs of points.
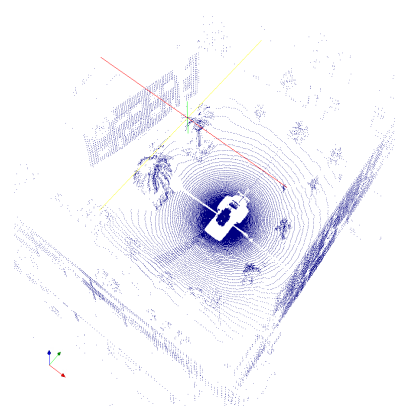4) Repeat steps 1-3 until all elements of the Hessian matrix H are calculated.

The second order partial derivatives for the Hessian matrix H are calculated numerically using finite differences.
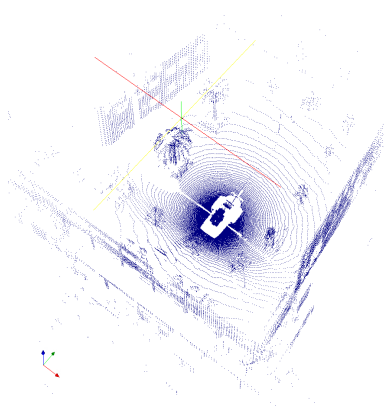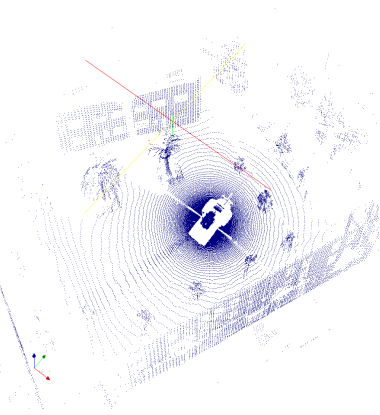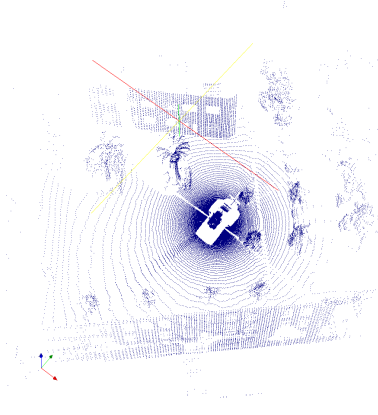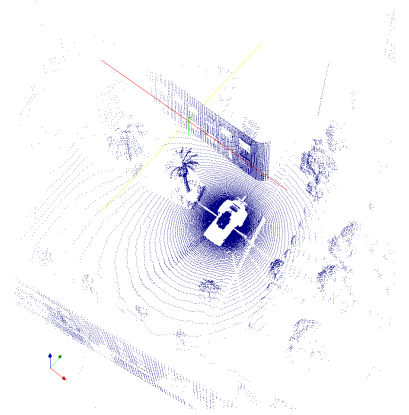
Fig. 2. Outdoor setting in (a) and 3D scans taken in (b)-(f) using the 3D data acquisition system presented in Section II.

V. Experimental Evaluation

In this section we present experimental results showing the performance of the 3D data acquisition system in outdoor environments. The images shown in Figure 2 present scans taken in the outdoor area near the ACFR building using the system described in Section II under a "move-sense-move" approach. The vehicle moved along the area, stopping every several meters and taking full 3D scans in each of these stops. As can be appreciated from the images, the scans contain a large amount of information, clearly delineating the environment structure and its obstacles, even in long ranges.

Figure 3 presents the aligned scans resulting from the 3D registration using the scan matching procedure described in Section III. The registration process was enriched using information given by dead-reckoning sensors. For this we proposed starting poses provided by the integration of steering-velocity encoders and IMU [19] in order to initialize the ICP procedure near the actual solution. In this way we were able to reduce the convergence times of the registration procedure while minimizing the risks of getting stuck in local minima. This figure shows all the superimposed tranformed scans

(using the registration vectors) that correspond to the images of Figure 2. This image was assembled in the coordinate frame of the first scan.

Figure 4 shows the results of implementing the previous concepts in a "non-stop" incremental fashion. The approach is an extension to 3D of the Scan-SLAM mechanism presented in [20] for planar maps. Here, continuous observations were obtained by the registration of sucessive full 3D scans using scan matching and an estimation of the registration errors, as shown previously in Section III and Section IV.

VI. Conclusions and Future Work

This paper presented the deployed sensory system for 3D environmental sensing in outdoor environments. The 3D data acquisition architecture was described, and techniques for the registration of 3D scans and for the estimation of their errors were analyzed. As illustrated through experiments, the system performs robustly and accurately in real outdoor environments, providing scans of good quality that can be assembled into larger maps consistently. The availability of dead-reckoning sensors on the experimental platform (steering-velocity en-
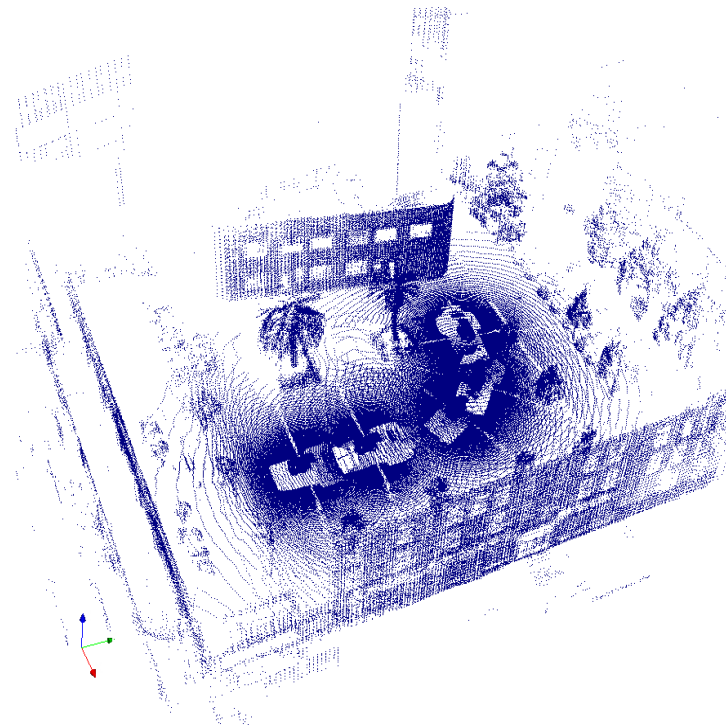
Fig. 3. Image showing the results of the 3D registration using scan matching. This image presents all the superimposed aligned scans that correspond to the images of Figure 2.

coders and IMU) provided extra means for accelerating the 3D registration mechanism while reducing the possibility of falling in undesired local minima.

The possibility of estimating the covariance of the registration permits the use of the 3D registration pose in a probabilistic framework. This, in fact, permits the expansion of the Scan-SLAM architecture proposed in [20] to 3D mapping representations. We are currently further improving our architecture in two directions. Firstly, we are extending the system to a dynamic scanning framework, in order to be able to fuse scans taken with the moving vehicle at high speeds and considering the inherent distortion. And secondly, we are integrating the 3D laser range finder with a camera, augmenting to 3D the concept camera-laser calibration approach presented in [21] for 2D lasers.

VII. ACKNOWLEDGMENTS

REFERENCES

[1] J. J. Leonard and H. F. Durrant-Whyte, "Simultaneous Map Building and Localization for an Autonomous Mobile Robot," in *IEEE/RSJ International Workshop on Intelligent Robots and Systems*. Osaka, Japan: IEEE, 1991.

[2] M. Dissanayake, P. Newman, S. Clark, H. Durrant-Whyte, and M. Csorba, "A Solution to the Simultaneous Localisation and Map Building (SLAM) Problem," *IEEE Transactions on Robotics and Automation*, vol. 17, no. 3, pp. 229–241, 2001.

[3] J. E. Guivant and E. M. Nebot, "Optimization of the Simultaneous Localization and Map-building Algorithm for Real-time Implementation," *IEEE Transactions on Robotics and Automation*, vol. 17, no. 3, pp. 242–257, 2001.

[4] S. Thrun, W. Burgard, and D. Fox, "A real-time algorithm for mobile robot mapping with application to multi-robot and 3D mapping," in *International Conference on Robotics and Automation*. San Francisco, California: IEEE, 2000.

[5] P. Jensfelt and H. I. Christensen, "Pose tracking using laser scanning and minimalistic environmental models," *IEEE Transactions on Robotics and Automation*, vol. 17, no. 2, pp. 138–147, 2001.

[6] H. Surmann, A. Nüchter, and J. Hertzberg, "An Autonomous Mobile Robot with a 3D Laser Range Finder for 3D Exploration and Digitalization of Indoor Environments," *Robotics and Autonomous Systems*, vol. 45, no. 1, pp. 181–198, 2003.

[7] D. Cole, A. Harrison, and P. Newman, "Using Naturally Salient Regions for SLAM with 3D Laser Data," in *International Conference on Robotics and Automation, SLAM Workshop*. Barcelona, Spain: IEEE, 2005.

[8] T. Bailey, "Mobile Robot Localisation and Mapping in Extensive Outdoor Environments," PhD thesis, University of Sydney, Australia, 2002.

[9] O. Bengtsson and A.-J. Baerveldt, "Robot Localization based on Scan–matching – Estimating the Covariance Matrix for the IDC Algorithm," *Robotics and Autonomous Systems*, vol. 44, no. 1, pp. 29–40, 2003.
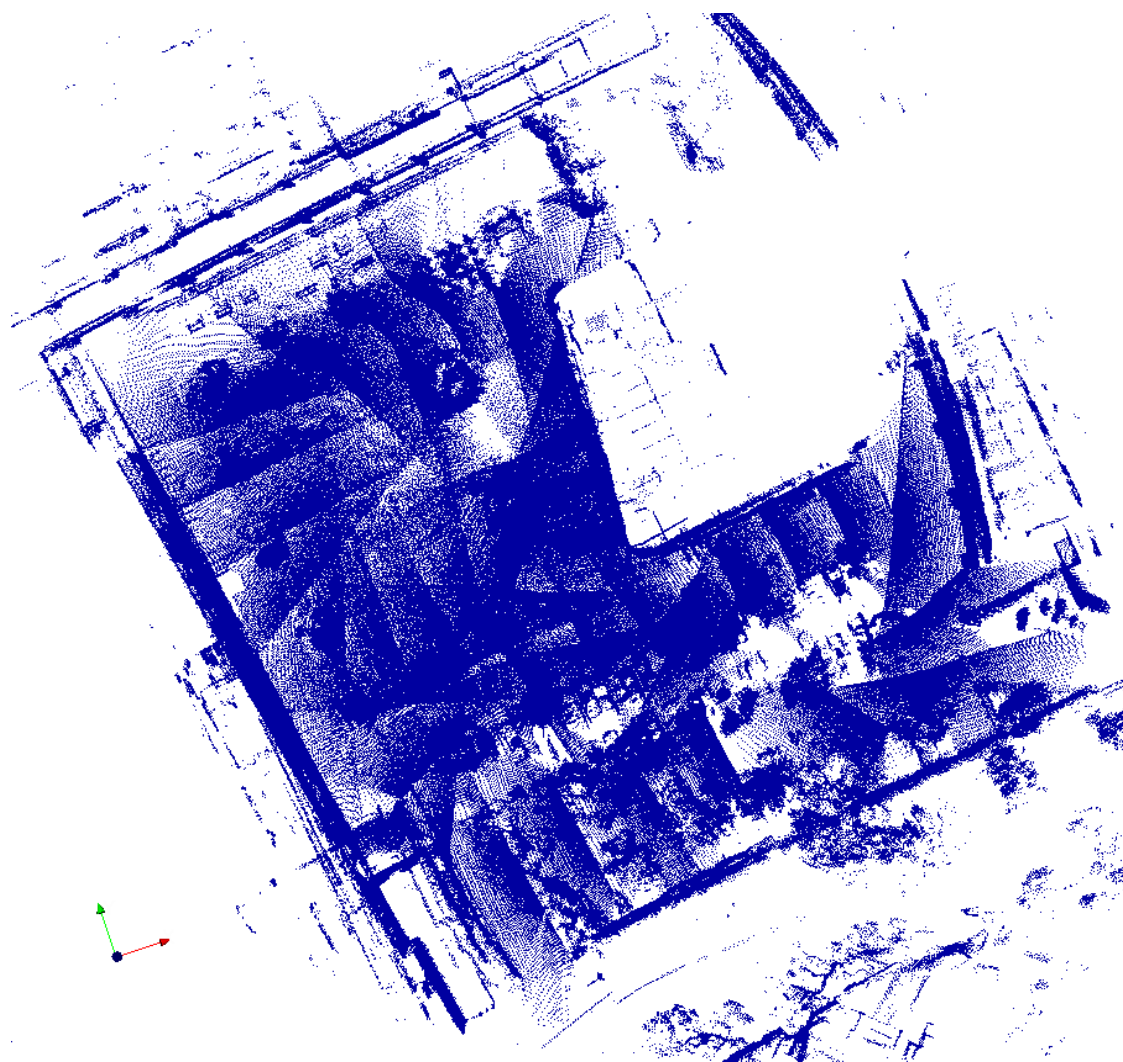
Fig. 4. Image showing a map obtained through the implementation of the full 3D SLAM algorithm (Scan-SLAM).

[10] Sick, "Sick Lase Data Sheets," http://www.sick.de/de/en.html, 2005.

[11] QNX, "QNX Programmer's Guide," http://www.qnx.com/, 2005.

[12] B. Horn, "Closed-form Solution of Absolute Orientation using Unit Quaternions," *Journal of the Optical Society of America A*, vol. 4, no. 4, pp. 629–642, 1987.

[13] P. Besl and N. McKay, "A Method for Registration of 3-D Shapes," *IEEE Transactions on Pattern Analysis and Machine Intelligence*, vol. 14, no. 2, pp. 239–256, 1992.

[14] F. Lu and E. Milios, "Robot Pose Estimation in Unknown Environments by Matching 2D Range Scans," *Journal of Intelligent and Robotic Systems*, vol. 18, pp. 249–275, 1997.

[15] Z. Xiong and M. Y. Wang, "A Near–Optimal Probing Strategy for Workpiece Localization," *IEEE Transactions on Robotics and Automation*, vol. 20, no. 4, pp. 668–676, 2004.

[16] M. Y. Wang, "An Optimum Design for 3D Fixture Synthesis in a Point Set Domain," *IEEE Transactions on Robotics and Automation*, vol. 16, no. 6, pp. 839–846, 2000.

[17] C. H. Menq, H. T. Yau, and G. Y. Lai, "Automated Precision Measurement of Surface Profile in CAD Directed Inspection," *IEEE Transactions on Robotics and Automation*, vol. 8, no. 2, pp. 268–278, 1992.

[18] S. M. Kay, *Fundamentals of Statistical Signal Processing – Estimation Theory*. New Jersey: Prentice–Hall, 1993.

[19] E. Nebot and H. Durrant-Whyte, "Initial Calibration and Alignment of Low Cost Inertial Navigation Units for Land Vehicle Applications," *Journal of Robotics Systems*, vol. 16, no. 2, pp. 81–92, 1999.

[20] J. Nieto, T. Bailey, and E. Nebot, " Scan-SLAM: Combining EKF-SLAM and Scan Correlation," in *International Conference on Robotics and Automation, SLAM Workshop*. Barcelona, Spain: IEEE, 2005.

[21] Q. Zhang and R. Pless, "Extrinsic Calibration for a Camera and Laser Ranger Finder (improves camera intrinsic claibration)," in *IEEE/RSJ International Workshop on Intelligent Robots and Systems*. Japan: IEEE, 2004.